ACCELERATED PUBLICATION

This paper is available online at www.jbc.org

THE JOURNAL OF BIOLOGICAL CHEMISTRY VOL. 284, NO. 43, pp. 29246–29250, October 23, 2009

Mal3 Masks Catastrophe Events in *Schizosaccharomyces pombe* Microtubules by Inhibiting Shrinkage and Promoting Rescue*[S]

Received for publication, August 4, 2009, and in revised form, September 6, 2009
Published, JBC Papers in Press, September 9, 2009, DOI 10.1074/jbc.C109.052159

Miho Katsuki, Douglas R. Drummond, Michael Osei, and Robert A. Cross[1]

From the Molecular Motors Group, Marie Curie Reaerch Institute, Oxted, Surrey RH8 0TL, United Kingdom

Schizosaccharomyces pombe **Mal3 is a member of the EB family of proteins, which are proposed to be core elements in a tip-tracking network that regulates microtubule dynamics in cells. How Mal3 itself influences microtubule dynamics is unclear. We tested the effects of full-length recombinant Mal3 on dynamic microtubules assembled *in vitro* from purified *S. pombe* tubulin, using dark field video microscopy to avoid fluorescent tagging and data-averaging techniques to improve spatiotemporal resolution. We find that catastrophe occurs stochastically as a fast (<2.2 s) transition from constant speed growth to constant speed shrinkage with a constant probability that is independent of the Mal3 concentration. This implies that Mal3 neither stabilizes nor destabilizes microtubule tips. Mal3 does, however, stabilize the main part of the microtubule lattice, inhibiting shrinkage and increasing the frequency of rescues, consistent with recent models in which Mal3 on the lattice forms stabilizing lateral links between neighboring protofilaments. At high concentrations, Mal3 can entirely block shrinkage and induce very rapid rescue, making catastrophes impossible to detect, which may account for the apparent suppression of catastrophe by Mal3 and other EBs *in vivo*. Overall, we find that Mal3 stabilizes microtubules not by preventing catastrophe at the microtubule tip but by inhibiting lattice depolymerization and enhancing rescue. We argue that this implies that Mal3 binds microtubules in different modes at the tip and on the lattice.**

Microtubules are intrinsically dynamic self-assembling structures of tubulin subunits (1) whose polymerization is subject to extensive spatial and temporal control in cells partly through the activity of microtubule-associated proteins (2). In cells, the EB family of microtubule plus end-tracking proteins (+TIPs)[2] localizes at the plus end of growing but not shrinking microtubules. EB depletion increases catastrophe frequency and reduces microtubule length in many species (3–5), suggesting that EBs suppress microtubule catastrophes. It is, however, unclear from these cellular studies whether this activity is direct or indirect because the dynamic binding of EBs to other +TIPs proteins enhances the localization of all EB complex proteins, including EB1, to microtubule ends (6).

To determine the direct effect of EB family proteins on microtubule dynamics, *in vitro* experiments are necessary. These have established that microtubule end tracking is an intrinsic property of the EB proteins and that other +TIP proteins such as CLIP170 are dependent upon EBs for their microtubule end localization (7–9). However, EB1 binding also directly alters the structure of growing microtubule tips (10). *In vitro* studies show that Mal3, the EB1 homologue in *Schizosaccharomyces pombe*, can also affect the structure of microtubules. Sandblad *et al.* (11) found localization of Mal3 along the (A-lattice) seam of B-lattice microtubules and proposed this as a potential mechanism for direct microtubule stabilization by the EBs. Des Georges *et al.* (12) showed that Mal3 binds to and specifically stabilizes the A-lattice protofilament overlap, promoting nucleation and assembly of A-lattice-containing microtubules.

Several studies *in vitro* have all shown that EBs can affect microtubule dynamics (4, 7, 10, 13) but conflict over which parameter is affected. Thus although Bieling *et al.* (7) and Manna *et al.* (13) observed no effect on microtubule growth rates, Komarova *et al.* (4) and Vitre *et al.* (10) found an acceleration of growth. Manna *et al.* (13) found that EB1 inhibits catastrophe, yet the other studies observed that EBs trigger catastrophe events. There is clearly a need to resolve these apparent conflicts, especially as the same proteins *in vivo* appear to suppress catastrophe.

To try to elucidate the mechanism by which EB proteins influence microtubule assembly, we developed a minimalist approach in which the potential for confounding factors to affect the data is reduced or eliminated. Our assay uses proteins from a single organism, *S. pombe*, and GMPCPP-stabilized microtubule seeds assembled from purified tubulin with only the seeds attached to the chamber surface. We used this system to measure the effects of unlabeled full-length Mal3 on the polymerization dynamics of unlabeled *S. pombe* microtubules. Microtubules were imaged using dark field microscopy to avoid fluorescent labeling (see Fig. 1*A*). We also developed a semiautomated analysis system that allows us to digitize a large number of events, which can then be processed by data averaging and filtering. This reduces noise, allowing us to examine the detailed kinetics of the catastrophic switch from growth to shrinkage. Using this system, we find that Mal3 has no direct

* This work was supported by grants from Cancer Research UK (Grant C19638/A6211), the Association for International Cancer Research (Grant 09-0221), the Medical Research Council (Grant G0200542), and Marie Curie Cancer Care.

[S] The on-line version of this article (available at http://www.jbc.org) contains supplemental methods and references, Figs. 1–3, Table 1, and three movies.

[1] To whom correspondence should be addressed: The Chart, Oxted, Surrey RH8 0TL, UK. Tel.: 44-1883-722-306 (ext. 219); Fax: 44-1883-714-375; E-mail: r.cross@mcri.ac.uk.

[2] The abbreviations used are: +TIPs, microtubule plus end-tracking proteins; GMPCPP, guanosine 5′-(α,β-methylenetriphosphate); Pipes, 1,4-piperazinediethanesulfonic acid.

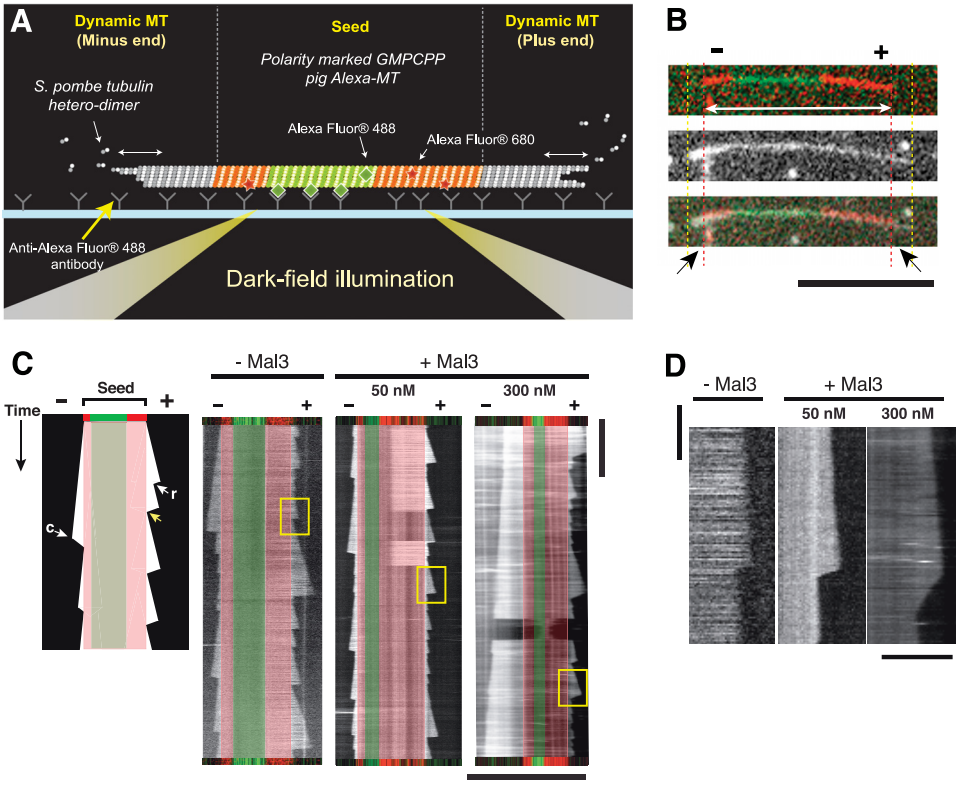

FIGURE 1. ***In vitro S. pombe* microtubule dynamics assay.** *A*, schematic diagram of *S. pombe* microtubule dynamics assay. GMPCPP stabilized polarity-marked microtubule seed assembled from Alexa Fluor 488- and Alexa Fluor 680-labeled pig brain tubulin. Only the center of the seed is attached to the surface by anti-Alexa Fluor 488 antibody. Dynamic non-fluorescently labeled *S. pombe* microtubules grown from seeds were observed by dark field illumination. *B*, merged fluorescence images of GMPCPP stabilized, polarity-marked pig microtubule seed (*pig Alexa-MT*). *Green*, Alexa Fluor 488; *red*, Alexa Fluor 680. Polarity is indicated by − or +. The plus end of the seed has a longer Alexa Fluor 680-labeled region (*upper panel*), a dark field image showing pig microtubule seed plus elongated *S. pombe* microtubules (*middle panel*), and the merged images (*lower panel*). *Red broken lines* show the ends of the seed, and *yellow broken lines* show the ends of the elongated *S. pombe* microtubules. *Arrows* indicate the dynamic *S. pombe* microtubule elongated from the stabilized microtubule seed. *Scale bar*: 10 μm. *C*, kymographs of microtubule length change over time. The *left panel* shows a diagram of a typical example. Time is indicated by the *vertical axis*, and length is indicated by the *horizontal axis*. Rescue (*r*) and catastrophe (*c*) events are labeled. Regrowth of shrinking microtubules from the seed (*yellow arrow*) were not counted as rescues. *Scale bars*: *vertical*, 5 min; *horizontal*, 20 μm. + and − ends of microtubule are indicated. *D*, enlargement of catastrophe events from the *yellow rectangle* in *C*. *Scale bars*: *vertical*, 30 s; *horizontal*, 5 μm.

effect upon the frequency or kinetics of catastrophe events but that it does reduce shrinkage rates and increase rescue frequency in a dose-dependent manner.

EXPERIMENTAL PROCEDURES

Protein Preparations—*S. pombe* single isoform tubulin and Mal3 protein (Mal3-308) were prepared and concentrations determined as described in des Georges *et al.* (12). Pig brain tubulin was purified as described by Mitchison and Kirschner (14) and fluorescently labeled using Alexa Fluor 488 succinimidyl ester (A20000, Invitrogen) or Alexa Fluor 680 succinimidyl ester (A20008, Invitrogen) (15).

Microtubule Dynamics Assay—Polarity-marked GMPCPP microtubule seeds were attached by anti-Alexa Fluor 488 antibody (A11094, Invitrogen) to Sigmacote (Sigma)-coated coverglasses in flow cells. Dynamic non-labeled *S. pombe* microtubules were assembled by the addition of non-labeled 4.5 μM *S. pombe* single isoform tubulin in PEM buffer (100 mM Pipes, pH 6.9, 1 mM $MgSO_4$, 2 mM EGTA) (16) containing an oxygen-scavenging system (8 μg/ml catalase, 4.5 mg/ml glucose, 38 units/ml glucose oxidase, and 1% (v/v) 2-mercaptoethanol), 1 mM GTP, and 1 mM Mg-ATP. Fluorescent seeds were imaged by epifluorescence microscopy, and unlabeled microtubule dynamics were imaged by dark field microscopy in a temperature-regulated box at 25 ± 0.5 °C. Dark field images were captured at 1-s intervals during a 30-min incubation period using an electron-multiplying CCD camera (Andor, iXon^{EM}+ DU-897E).

Image Analysis—Kymographs were created from time-lapse images of dynamic microtubules using MetaMorph software (Molecular Devices). Kymographs of microtubule plus ends (n = 8–32 from 3–5 microtubules for each condition) were analyzed automatically using a custom macro for ImageJ (National Institutes of Health, Bethesda, MD) that detects the microtubule end in dark field kymograph images.

Data Processing—Catastrophe events were analyzed by superimposing and aligning different data sets from the automated tip tracking using a custom Excel macro. A median filter was then applied to remove outlying data points and noise using a custom Visual Basic for Applications (VBA) macro in Excel. All macros are available from the Marie Curie Research Institute Molecular Motors Group. See supplemental information for detailed methods.

RESULTS AND DISCUSSION

We examined the effect of Mal3 expressed in *Escherichia coli* on dynamic microtubules formed from highly purified single isoform *S. pombe* tubulin. Dynamic microtubules polymerized from immobilized, polarity-marked seeds assembled from pure tubulin were imaged by dark field microscopy (17) (Fig. 1*B*; supplemental movies). Kymographs were generated (Fig. 1, *C* and *D*), and an automated tracking program was developed to digitize the microtubule end position (see the supplemental methods). Plots of microtubule end position against time were analyzed to determine microtubule growth and shrinkage rates and catastrophe and rescue frequencies, which together define microtubule dynamics (Fig. 2*A*; Table 1). Measurements were repeated over a range of Mal3 concentrations.

We find that microtubules containing *S. pombe* single isoform tubulin grow at 0.5 μm/min (Fig. 2*A*; Table 1) compared with 3 μm/min *in vivo* (18). The addition of Mal3 at up to

500 nM does not alter this growth rate. Catastrophe frequency was determined from a large number of events (43–80 events during 103–140 min of microtubule growth) and remained constant at 0.5 min^{-1} over the full range of Mal3 concentrations tested (Fig. 2*A*; Table 1).

Because Mal3 *in vivo* is reported to suppress catastrophe, we examined the intrinsic kinetics of *in vitro* catastrophe in more detail to determine whether Mal3 alters the time course of catastrophe rather than simply the frequency. For each Mal3 concentration, 8–32 subsets of catastrophe events suitable for further analysis were identified (supplemental Table 1), excised from the primary data, superimposed, and optimally aligned using a recursive procedure (see the supplemental methods). The final aligned data were median-filtered to reduce noise (supplemental Fig. S1). This image-processing procedure reveals the catastrophe event under unloaded conditions with unprecedented spatiotemporal resolution (Fig. 2*B*). Although Schek *et al.* (19) previously tracked the dynamics of catastrophe at high resolution, their method requires exertion of force on the microtubule tip, which can alter the dynamics.

Our methods detect catastrophes as rapid transitions from steady growth to steady shrinkage with no intermediate states such as pauses, at all Mal3 concentrations assayed (Fig. 2*B*). By eye, transition from steady growth to steady shrinkage appears to occur within 1 s or so, at all concentrations of Mal3 (Fig. 2*B*). Plotting of the regions enclosing 95% of the data points for the median-filtered growth and shrinkage data provides a formal specification for the transition between growth and shrinkage (supplemental Fig. S2). The overlap of these regions creates a zone around the catastrophe event where data points could belong to either growth or shrinkage regions or to some other transitional phase. The minimum physical extent we measure for this indeterminate zone is 64 nm (at 300 nM Mal3), whereas its minimum duration is 2.2 s (at 0 nM Mal3). These values represent upper limits for the spatiotemporal extent of the catastrophe zone.

Tip tracking by Mal3 on brain microtubules is observed *in vitro* in conditions similar to our assay (7). Thus although we do not directly visualize Mal3, we infer that tip

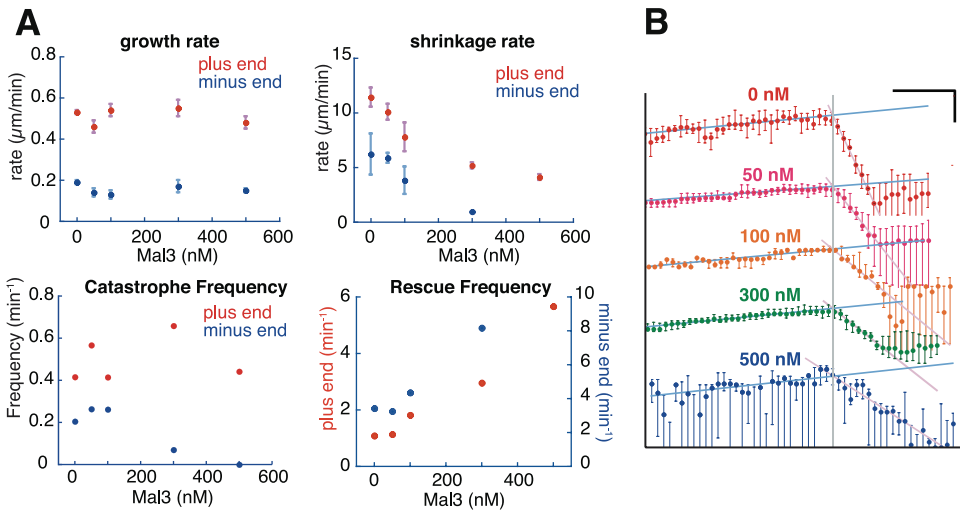

FIGURE 2. **Mal3 effects on microtubule dynamics.** *A*, microtubule plus and minus end dynamic parameters in 4.5 μM *S. pombe* tubulin and various concentrations of Mal3 (0–500 nM). *Error bars* indicate S.E. *B*, transition from growth to shrinkage during catastrophe events at plus ends in the presence of 0–500 nM Mal3. For each Mal3 concentration, plots of microtubule length against time were superimposed and aligned by automated fits, and the median was determined. *Error bars* show upper and lower quartiles of the data. *Scale bars*: *horizontal*, 10 s; *vertical*, 0.5 μm.

TABLE 1

Mal3 effect on microtubule dynamics

Data shows mean ± S.D. Catastrophe events were defined as transitions between periods of continuous growth lasting longer than 20 s and periods of shrinkage longer than 3 s. Catastrophe and rescue frequencies were calculated by dividing the total number of events by the total time spent in growth and shrinkage (growth time, shrinkage time); respectively. *n* represents the total number of events observed. NA, not applicable (since no catastrophe events were observed).

Mal3	Growth rate	Shrinkage rate	Catastrophe frequency	Rescue frequency	Growth time	Shrinkage time
nM	*μm/min*	*μm/min*	*events/min*	*events/min*	*min*	*min*
Plus end						
0	0.53 ± 0.13	11.4 ± 4.0	0.416	1.09	127.4	3.67
	n = 90	*n* = 21	*n* = 53	*n* = 4		
50	0.46 ± 0.20	10.1 ± 4.6	0.567	1.14	141.08	3.52
	n = 64	*n* = 39	*n* = 80	*n* = 4		
100	0.54 ± 0.15	7.8 ± 4.2	0.415	1.82	103.5	2.75
	n = 29	*n* = 10	*n* = 43	*n* = 5		
300	0.55 ± 0.21	5.2 ± 1.6	0.659	2.96	113.75	9.47
	n = 33	*n* = 34	*n* = 75	*n* = 28		
500	0.48 ± 0.13	4.1 ± 1.2	0.442	5.67	122.08	8.47
	n = 21	*n* = 20	*n* = 54	*n* = 48		
Minus end						
0	0.19 ± 0.06	6.2 ± 5.7	0.205	3.43	136.43	2.33
	n = 32	*n* = 9	*n* = 28	*n* = 8		
50	0.14 ± 0.08	5.9 ± 1.7	0.264	3.26	140.32	1.25
	n = 29	*n* = 14	*n* = 37	*n* = 5		
100	0.13 ± 0.08	3.8 ± 5.3	0.262	4.36	114.37	0.92
	n = 23	*n* = 18	*n* = 30	*n* = 4		
300	0.17 ± 0.07	1.0	0.07	8.18	143.18	0.37
	n = 5	*n* = 2	*n* = 10	*n* = 3		
500	0.15 ± 0.02	NA	0	NA	137.82	0.06
	n = 4					

tracking Mal3 affects neither the frequency nor the intrinsic dynamics of catastrophe in *S. pombe* microtubules.

Although Mal3 does not influence catastrophe frequency, it does have a considerable effect on plus end dynamics, reducing shrinkage rates and increasing rescue frequencies following catastrophe in a dose-dependent manner (Fig. 2*A*; Table 1). Previously we showed that Mal3 binds the lattice of both brain and *S. pombe* microtubules with a 1:1 stoichiometry and $K_d \sim 1$ μM (12). We observe effects on shrinkage rates at Mal3 concentrations as low as 50 nM. With a K_d of 1 μM, Mal3 is predicted to occupy only about 4.6% of the lattice binding sites.

Mal3 increased the rescue frequency 6-fold over the range 0–500 nM Mal3 (Fig. 2*A*; Table 1). Rescues probably restore a protective cap of GTP tubulin heterodimers to the microtubule, blocking further shrinkage and allowing regrowth. Mal3 might directly promote the addition of GTP heterodimers; however, this mechanism seems unlikely as we see no effect of Mal3 on the growth rate of microtubules assembling from GTP heterodimers. Instead, we favor a model in which Mal3 is stabilizing the GDP lattice by linking protofilaments and inhibiting protofilament peeling so that GTP subunits can more easily add to the GDP lattice microtubule end. Thus the same protofilament-linking mechanism could account for the ability of sparsely distributed Mal3 to inhibit shrinkage and to promote rescues. Sparsely distributed GTP heterodimers within the lattice can also induce rescue events (20), potentially by a similar mechanism.

Mal3 tracks both the plus and the minus ends of microtubules *in vitro* (7), and just as at the plus end, Mal3 at the minus end has no effect on growth rate but slows shrinkage and promotes rescue in a dose-dependent fashion (Fig. 2*A*; Table 1). However, although Mal3 has no detectable effect on plus end catastrophe, it does appear to inhibit catastrophe at the minus end (Figs. 1*C* and 2*A*; Table 1; supplemental movies). Why does Mal3 apparently suppress catastrophe at minus ends but not at plus ends? Mal3 concentrations up to 100 nM do not inhibit the minus end catastrophe frequency, but higher Mal3 concentrations do, and 500 nM Mal3 reduces the rate to zero (Fig. 2*A*; Table 1). Strikingly, the suppression of minus end catastrophe was only observed at concentrations of Mal3 (>300 nM) that significantly suppress minus end shrinkage rates (<1.0 μm/min) and promote minus end rescue (>8.2 min^{-1}) (Table 1). Inhibition of shrinkage and promotion of rescues requires more Mal3 at the plus end than at the minus end where the dynamics are already biased toward reduced shrinkage and increased rescues; even 500 nM Mal3 only reduces plus end shrinkage rate to 5.7 μm/min and increases the rescue frequency to 4.1 min^{-1}.

We propose a model where Mal3 does not affect the catastrophe frequency itself. Instead, increasing Mal3 concentrations make catastrophes progressively harder to detect by reducing the rate of shrinkage and the duration of shrinkage events (Fig. 3, *A*–*C*) until it becomes essentially impossible to observe catastrophes. Our model envisages that the true catastrophe frequency is unaffected, even at high Mal3 concentrations, but that the *apparent* catastrophe frequency decreases.

Our model suggests that a sufficient increase in Mal3 concentration would cause the apparent suppression of all plus end

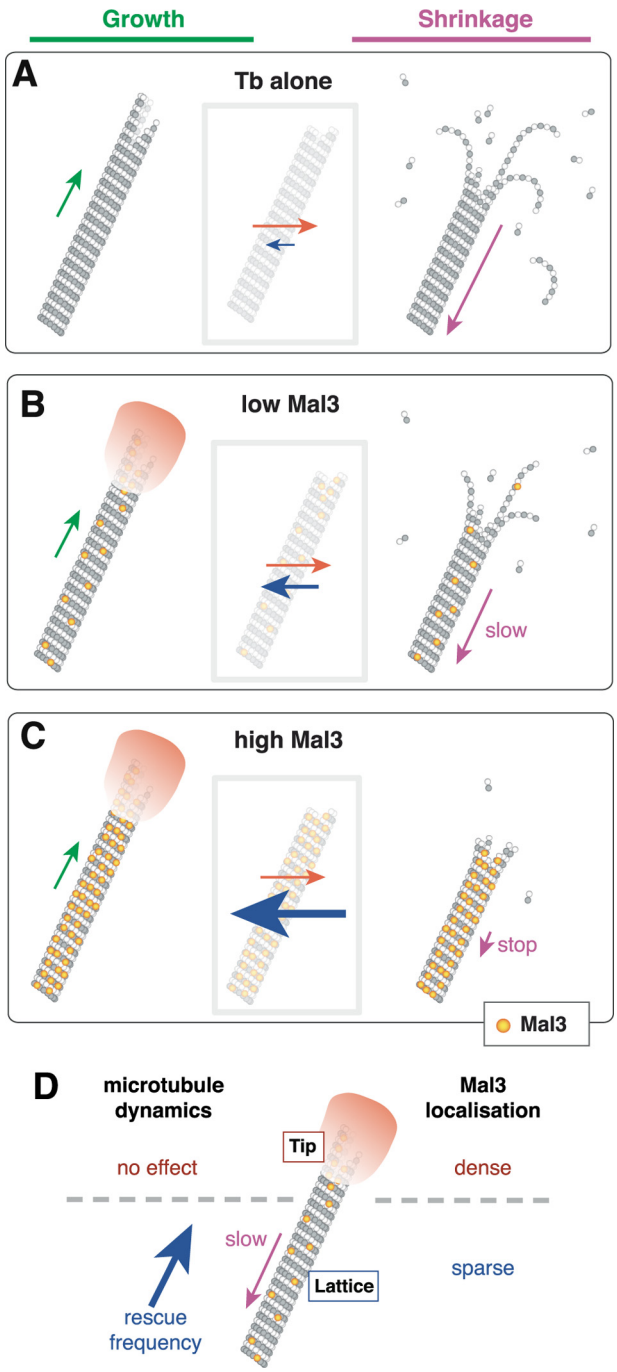

FIGURE 3. **Model for microtubule binding modes and the apparent suppression of microtubule catastrophe events by Mal3.** *A*, in the absence of Mal3, growing microtubules undergo frequent catastrophe (*red arrow*) and shrink rapidly (*violet arrow*) with occasional rescues (*blue arrow*). *B*, submicromolar concentrations of Mal3 do not alter growth rate (*green arrow*) or catastrophe frequency (*red arrow*) but do slow shrinkage (*violet arrow*) and increase rescue frequency by lateral cross-linking of protofilaments. *C*, at very high concentrations of Mal3, catastrophes still occur at the same rate but become impossible to detect because the shrinkage rate is effectively zero, whereas rescue events occur almost instantly. In all panels, *longer colored arrows* indicate higher rate constants. *D*, Mal3 binding modes. Mal3 has no effect on tip dynamics but does affect lattice dynamics, implying two different binding modes. Mal3 binds with high affinity at the tip of growing microtubules, giving rise to the characteristic EB family comet. Catastrophe results in loss of the tip binding mode and exposure of the lattice. Mal3 binds with lower affinity on the lattice, giving sparse decoration, but despite its lower affinity, this lattice-bound Mal3 stabilizes the lattice, forming lateral links between protofilaments and thereby slowing shrinkage and enhancing rescue. At sufficiently high concentrations of Mal3, these effects combine to give an apparent suppression of catastrophe events and continuous microtubule growth.

catastrophes. We were unable to test this prediction directly in the dynamics assay as higher concentrations of Mal3 caused too much spontaneous nucleation of microtubules. Therefore we used a protocol in which microtubules were preassembled and catastrophe events were induced by reducing the free tubulin concentration (supplemental Fig. S3). In the absence of Mal3, reducing the tubulin concentration from 7.5 to 3 μM resulted in immediate catastrophe followed by shrinkage to the stabilized seed boundary. However, reducing the tubulin concentration to 3 μM in the presence of 1 μM Mal3 stabilized the microtubules for over 30 min in a paused state with no change in microtubule length or catastrophe events observable (supplemental Fig. S3*B*). Subsequently flushing the chamber with 3 μM tubulin alone again caused immediate shrinkage (supplemental Fig. S3*C*). Thus at high concentrations, Mal3 can suppress shrinkage and (apparently) suppress catastrophes at the microtubule plus end, consistent with our model. At the minus end, we observe continuous growth without catastrophes or pausing because of the combined effects of reduced shrinkage and increased rescue frequencies. The similar Mal3 dose dependence of shrinkage rate reduction and rescue promotion suggests that these effects may arise from the same mechanism. We propose that Mal3 linking of protofilaments stabilizes the microtubule GDP lattice, inhibiting shrinkage and promoting rescue, leading to masking of catastrophe events.

Although like other EB family proteins Mal3 enriches at the tips of growing microtubules (7), this higher concentration of Mal3 at microtubule ends when compared with the lattice does not influence the dynamics of the microtubule end (Fig. 3*D*). We conclude that the Mal3 binding mode at the microtubule tip and on the lattice is different, perhaps because the tip is the only part of the microtubule composed of GTP heterodimers or because the tip is structurally different from the lattice (or both). It is paradoxical that the apparently higher affinity tip binding has no detectable effect on microtubule dynamics. One resolution of this paradox would be if Mal3 binding made GDP-containing tubulin heterodimers behave more like GTP heterodimers, slowing their detachment from the microtubule, whilst enhancing the probability of microtubule rescue by promoting attachment of GTP subunits. We previously proposed that the microtubule-nucleating activity of Mal3 (12) could be explained by Mal3 binding and stabilizing nascent sheets of heterodimers in a way analogous to its tip binding activity. Our present observations reveal that Mal3 does not stabilize tips, suggesting that the nucleating activity is more likely to arise from the lattice-stabilizing activity that we observe here.

How do our observations apply *in vivo*? The concentration of Mal3 in cells may be about 200-fold less than the tubulin concentration (11). Based on our own preliminary estimates of tubulin concentration within *S. pombe* cells (not shown), the *in vivo* Mal3 concentration may be a few tens of nM, suggesting a potentially limited role for the direct effect of Mal3 on microtubule dynamics. To account for the observed stabilization of growing microtubules by Mal3 *in vivo*, additional Mal3 binding partner proteins may be required to recruit sufficient Mal3 onto the lattice (13, 21–23). Alternatively, the stabilization of microtubules by Mal3 *in vivo* may be due to recruitment of Mal3 binding partners to the tips. By accumulating on microtubule tips without affecting their dynamics, Mal3 provides a neutral platform for the recruitment of an extensive list of binding partners. Further *in vitro* reconstitution experiments will be necessary to test the relative contribution of these two mechanisms.

REFERENCES

1. Desai, A., and Mitchison, T. J. (1997) *Annu. Rev. Cell Dev. Biol.* **13,** 83–117
2. Akhmanova, A., and Hoogenraad, C. C. (2005) *Curr. Opin. Cell Biol.* **17,** 47–54
3. Busch, K. E., and Brunner, D. (2004) *Curr. Biol.* **14,** 548–559
4. Komarova, Y., De Groot, C. O., Grigoriev, I., Gouveia, S. M., Munteanu, E. L., Schober, J. M., Honnappa, S., Buey, R. M., Hoogenraad, C. C., Dogterom, M., Borisy, G. G., Steinmetz, M. O., and Akhmanova, A. (2009) *J. Cell Biol.* **184,** 691–706
5. Tirnauer, J. S., Grego, S., Salmon, E. D., and Mitchison, T. J. (2002) *Mol. Biol. Cell* **13,** 3614–3626
6. Akhmanova, A., and Steinmetz, M. O. (2008) *Nat. Rev. Mol. Cell Biol.* **9,** 309–322
7. Bieling, P., Laan, L., Schek, H., Munteanu, E. L., Sandblad, L., Dogterom, M., Brunner, D., and Surrey, T. (2007) *Nature* **450,** 1100–1105
8. Bieling, P., Kandels-Lewis, S., Telley, I. A., van Dijk, J., Janke, C., and Surrey, T. (2008) *J. Cell Biol.* **183,** 1223–1233
9. Dixit, R., Barnett, B., Lazarus, J. E., Tokito, M., Goldman, Y. E., and Holzbaur, E. L. (2009) *Proc. Natl. Acad. Sci. U.S.A.* **106,** 492–497
10. Vitre, B., Coquelle, F. M., Heichette, C., Garnier, C., Chrétien, D., and Arnal, I. (2008) *Nature Cell Biology* **10,** 415–421
11. Sandblad, L., Busch, K. E., Tittmann, P., Gross, H., Brunner, D., and Hoenger, A. (2006) *Cell* **127,** 1415–1424
12. des Georges, A., Katsuki, M., Drummond, D. R., Osei, M., Cross, R. A., and Amos, L. A. (2008) *Nat. Struct. Mol. Biol.* **15,** 1102–1108
13. Manna, T., Honnappa, S., Steinmetz, M. O., and Wilson, L. (2008) *Biochemistry* **47,** 779–786
14. Mitchison, T., and Kirschner, M. (1984) *Nature* **312,** 232–237
15. Hyman, A., Drechsel, D., Kellogg, D., Salser, S., Sawin, K., Steffen, P., Wordeman, L., and Mitchison, T. (1991) *Methods Enzymol.* **196,** 478–485
16. Walker, R. A., O'Brien, E. T., Pryer, N. K., Soboeiro, M. F., Voter, W. A., Erickson, H. P., and Salmon, E. D. (1988) *J. Cell Biol.* **107,** 1437–1448
17. Horio, T., and Hotani, H. (1986) *Nature* **321,** 605–607
18. Drummond, D. R., and Cross, R. A. (2000) *Curr. Biol.* **10,** 766–775
19. Schek, H. T., 3rd, Gardner, M. K., Cheng, J., Odde, D. J., and Hunt, A. J. (2007) *Curr. Biol.* **17,** 1445–1455
20. Dimitrov, A., Quesnoit, M., Moutel, S., Cantaloube, I., Poüs, C., and Perez, F. (2008) *Science* **322,** 1353–1356
21. Browning, H., and Hackney, D. D. (2005) *J. Biol. Chem.* **280,** 12299–12304
22. Nakamura, M., Zhou, X. Z., and Lu, K. P. (2001) *Curr. Biol.* **11,** 1062–1067
23. Mimori-Kiyosue, Y., Grigoriev, I., Lansbergen, G., Sasaki, H., Matsui, C., Severin, F., Galjart, N., Grosveld, F., Vorobjev, I., Tsukita, S., and Akhmanova, A. (2005) *J. Cell Biol.* **168,** 141–153